

## Research Article

# A Perspective Approach to Study the Valency-Based Irregular Indices for Benzenoid Planar Octahedron Structures

Maria Singaraj Rosary,<sup>1</sup> Ammar Alsinai ,<sup>2</sup> Mohammad Kamran Siddiqui ,<sup>3</sup> and Hanan Ahmed <sup>4</sup>

<sup>1</sup>Department of Mathematics, Vel Tech High-Tech Dr. Rangarajan Dr. Sakunthala Engineering College, Chennai 600062, India

<sup>2</sup>Department of Mathematics, University of Mysore, Mysuru, India

<sup>3</sup>Department of Mathematics, COMSATS University Islamabad, Lahore Campus, Lahore, Pakistan

<sup>4</sup>Department of Mathematics, Ibb University, Ibb, Yemen

Correspondence should be addressed to Hanan Ahmed; hananahmed1a@gmail.com

Received 2 February 2023; Revised 12 March 2023; Accepted 28 March 2023; Published 11 April 2023

Academic Editor: Rajalakshmanan Eswaramoorthy

Copyright © 2023 Maria Singaraj Rosary et al. This is an open access article distributed under the Creative Commons Attribution License, which permits unrestricted use, distribution, and reproduction in any medium, provided the original work is properly cited.

The molecular topology and the chemical structures which are not regular perform a dominant character in designing the compound in connection with their physical and chemical properties. The study of topological descriptors of molecular structures is widely used in the field of cheminformatics, information technology, biomedical science, and many more. Numerous topological indices have been evolved in the theory of chemistry. Graphs which are not regular can be specified using irregular measures. In this article, we find some irregularity indices, which are useful in Quantitative structure activity relationship for benzenoid structures. Based on the exact analytic expressions, the numerical and graphical comparison for benzenoid structures is also provided.

## 1. Introduction

In chemical graph theory, latest innovation in graph theoretical models and simulation of molecular graphs are conducted by various researchers. They empower the researchers to develop a correlation between graph theory and chemical compounds. Also, the researches explain the physical and chemical properties like freezing point, solubility, and melting point of chemical structure of various compounds [1–3]. An irregularity index is an analytical value associated with a chemical structure that describes a structure's irregularity. Von Collatz and Ulrich defined the notion “network irregularity” in 1957 [4]. Irregularity measures are aided to denote various organizations in convoluted networks. Self-similarity, network motif, and scale-freeness are all main topological features of these organizations [5].

Let  $\sigma((V(\sigma), X(\sigma)))$  be an ordered pair of graphs, where  $V(\sigma)$  is a nonempty vertex set and  $X(\sigma)$  is an edge set.

Topological descriptors can be obtained from the molecular structure. They are very helpful to explain Quantitative Structure Activity Relationship (QSAR) of medicines and chemical compounds to form their molecular characteristics by computing numerically [6].

The total number of edges incident with vertex  $m$  is called the degree of vertex  $l$ , it is denoted by  $\mathfrak{F}(l)$ . In a graph, the maximum vertex degree is denoted by  $\Delta(\sigma)$ . Topological study of Line graph of Remdesivir Compound used in the treatment of corona virus is discussed [7]. Degree-based topological indices and polynomials of hyaluronic acid-curcumin conjugates, locating and Multiplicative Locating Indices of Graphs with QSPR Analysis, and structural determination of Paraffin Boiling Points are well studied [3, 8–12]. Graph Irregularity Indices used as Molecular Descriptors in QSPR studies and Randic Index, Irregularity, and complex biomolecular networks are also extensively discussed [13, 14]. The expected values of arithmetic bond connectivity and geometric indices in random phenylene

chains are clearly presented [15–22]. In literature, Irregularity indices of metal organic frameworks [23], Bismuth Triiodide [24], probabilistic neural network [25], and computer networks like silicate, oxide, hexagonal, and honeycomb [26] were extensively studied. Gutman studied the topological indices and irregularity measures [27]. Graphs with equal irregularity indices are well explained [28]. Irregularity indices based on Zagreb indices were studied [29]. For line graph of Dutch windmill graph, the irregularity indices were extensively studied [30]. Several irregularity indices of Dendrimers structures were clearly discussed [31].

In this article, we compute the irregularity degree based topological indices of the benzenoid planar octahedron networks and compare the results graphically.

In 1972, Gutman discussed the first and second Zagreb indices [32].

$$\begin{aligned} M_1(\sigma) &= \sum_{lm \in X(\sigma)} (\mathfrak{F}(l) + \mathfrak{F}(m)), \\ M_2(\sigma) &= \sum_{lm \in X(\sigma)} (\mathfrak{F}(l) \times \mathfrak{F}(m)). \end{aligned} \quad (1)$$

In a graph, if all the degrees are same, then the graph is called a regular graph. Otherwise, it is irregular. The selected irregularity indices for benzenoid planar octahedron networks are represented by

$$\text{VAR}(\sigma) = \frac{M_1(\sigma)}{q} - \left(\frac{2p}{q}\right)^2,$$

$$\text{AL}(\sigma) = \sum_{lm \in X(\sigma)} |\mathfrak{F}(l) - \mathfrak{F}(m)|,$$

$$\text{IR1}(\sigma) = F(\sigma) - \left(\frac{2p}{q}\right)M_1(\sigma),$$

$$\text{IR2}(\sigma) = \sqrt{\frac{M_2(\sigma)}{p}} - \left(\frac{2p}{q}\right),$$

$$\text{IRF}(\sigma) = F(\sigma) - 2M_2(\sigma),$$

$$\text{IRFW}(\sigma) = \frac{\text{IRF}(\sigma)}{M_2(\sigma)},$$

$$\text{IRA}(\sigma) = \sum_{lm \in X(\sigma)} \left( (\mathfrak{F}(l))^{-1/2} - (\mathfrak{F}(m))^{-1/2} \right)^2,$$

$$\text{IRB}(\sigma) = \sum_{lm \in X(\sigma)} \left( (\mathfrak{F}(l))^{1/2} - (\mathfrak{F}(m))^{1/2} \right)^2,$$

$$\text{IRC}(\sigma) = \sum_{lm \in X(\sigma)} \frac{\sqrt{\mathfrak{F}(l)\mathfrak{F}(m)}}{p} - \frac{2p}{q},$$

$$\text{IRDIF}(\sigma) = \sum_{lm \in X(\sigma)} \left| \frac{\mathfrak{F}(l)}{\mathfrak{F}(m)} - \frac{\mathfrak{F}(m)}{\mathfrak{F}(l)} \right|,$$

$$\begin{aligned} \text{IRL}(\sigma) &= \sum_{lm \in X(\sigma)} |\ln \mathfrak{F}(l) - \ln \mathfrak{F}(m)|, \\ \text{IRLU}(\sigma) &= \sum_{lm \in X(\sigma)} \frac{|\mathfrak{F}(l) - \mathfrak{F}(m)|}{\min(\mathfrak{F}(l), \mathfrak{F}(m))}, \\ \text{IRLF}(\sigma) &= \sum_{lm \in X(\sigma)} \frac{|\mathfrak{F}(l) - \mathfrak{F}(m)|}{\sqrt{\mathfrak{F}(l)\mathfrak{F}(m)}}, \\ \text{IRLA}(\sigma) &= 2 \sum_{lm \in X(\sigma)} \frac{|\mathfrak{F}(l) - \mathfrak{F}(m)|}{\mathfrak{F}(l) + \mathfrak{F}(m)}, \\ \text{IRGA}(\sigma) &= \sum_{lm \in X(\sigma)} \ln \frac{\mathfrak{F}(l) + \mathfrak{F}(m)}{2\sqrt{\mathfrak{F}(l)\mathfrak{F}(m)}} \end{aligned} \quad (2)$$

## 2. Main Outcomes

The structure of Benzenoid planar octahedron is constructed and the topological properties of this structure is well discussed [33]. The 2-dimensional structure of Benzenoid planar octahedron structure is given in Figure 1. We represent the graph of Benzenoid planar octahedron by  $\sigma_n$ ,  $n \geq 2$ , where  $n$  denotes the dimension of Benzenoid planar octahedron. Figure 1 depicts the 2-dimensional structure of the molecular graph of  $\sigma_2$ . The total number of vertices ( $q$ ) and edges ( $p$ ) in the structure of Benzenoid planar octahedron are  $45n^2 - 3n$  and  $90n^2$ .

The set of edges of Benzenoid planar octahedron structure is divided into five partitions based on the degree of end vertices. The first edge partition includes of  $36n^2$  edges  $lm$ , where  $\mathfrak{F}(l) = 3$  and  $\mathfrak{F}(m) = 3$ . The second edge partition includes of  $12n$  edges  $lm$ , where  $\mathfrak{F}(l) = 3$  and  $\mathfrak{F}(m) = 4$ . The third edge partition includes of  $36n^2 - 12n$  edges  $lm$ , where  $\mathfrak{F}(l) = 3$  and  $\mathfrak{F}(m) = 8$ . The fourth edge partition includes of  $12n$  edges  $lm$ , where  $\mathfrak{F}(l) = 4$  and  $\mathfrak{F}(m) = 8$ . The fifth edge partition includes of  $18n^2 - 12n$  edges  $lm$ , where  $\mathfrak{F}(l) = 8$  and  $\mathfrak{F}(m) = 8$ . Table 1 shows the edge partition of Benzenoid planar octahedron structure.

Now the irregularity degree based topological indices is computed as.

**Theorem 1.** We consider the graph  $\sigma_n$ ,  $n \geq 2$ , then the irregularity indices of Benzenoid planar octahedron structure are

$$\text{VAR}(\sigma_n) = \frac{4(225n^2 - 195n + 8)}{(1 - 15n)^2},$$

$$\text{AL}(\sigma_n) = 180n^2 - 12n,$$

$$\text{IR1}(\sigma_n) = -3600n^6 + 384n^5 + 2700n^3 + 5292n^2 - 1152n,$$

$$\text{IR2}(\sigma_n) = \sqrt{\frac{2}{15}} \sqrt{n^3(195n - 44)} + \frac{60n}{1 - 15n},$$

$$\text{IRF}(\sigma_n) = 900n^2 - 96n,$$

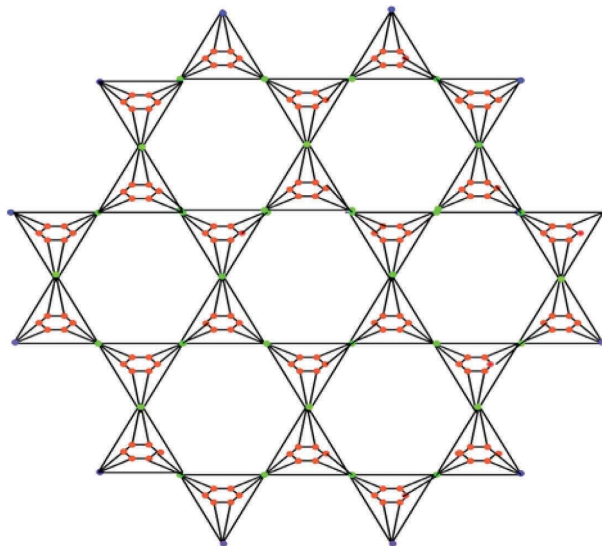


FIGURE 1: Benzenoid planar octahedron structure of dimension 2.

TABLE 1: Edge partition of benzenoid planar octahedron structure.

$(\mathfrak{I}(l), \mathfrak{I}(m))$	(3, 3)	(3, 4)	(3, 8)	(4, 8)	(8, 8)
Number of edges	$36n^2$	$12n$	$36n^2 - 12n$	$12n$	$18n^2 - 12n$

$$\text{IRFW}(\sigma_n) = \frac{900n^2 - 96n}{2340n^2 - 528n},$$

$$\text{IRA}(\sigma_n) = 1.8030n^2 - 0.2718n,$$

$$\text{IRB}(\sigma_n) = 43.2734n^2 - 5.3274n,$$

$$\text{IRC}(\sigma_n) = \frac{428.36n - 45.345}{90n} - \frac{60n}{15n - 1},$$

$$\text{IRDIF}(\sigma_n) = 82.5n^2 - 2.5n,$$

$$\text{IRL}(\sigma_n) = 35.3088n^2 - 0.0012n,$$

$$\text{IRLU}(\sigma_n) = 4n(15n - 1),$$

$$\text{IRLF}(\sigma_n) = 36.74n^2 - 0.29769n,$$

$$\text{IRLA}(\sigma_n) = 32.7272n^2 + 0.5195n, \quad (3)$$

$$\text{IRGA}(\sigma_n) = 4.16592n^2 - 0.55824n.$$

*Proof.* Applying the partition of edges of end vertices of each edge of the Benzenoid planar octahedron structure  $\sigma_n$  exploited in Table 1, we calculate the irregularity indices of the Benzenoid planar octahedron structure  $\sigma_n$  and the mathematical computations are given as follows:

$$\text{VAR}(\sigma_n) = \frac{M_1(\sigma_n)}{q} - \left(\frac{2p}{q}\right)^2 = \frac{900n^2 - 96n}{45n^2 - 3n} - \left(\frac{2(90n^2)}{45n^2 - 3n}\right)^2 = \frac{4(225n^2 - 195n + 8)}{(1 - 15n)^2},$$

$$\begin{aligned} \text{AL}(\sigma_n) &= \sum_{lm \in X(\sigma)} |\mathfrak{I}(l) - \mathfrak{I}(m)| = |3 - 3|36n^2 + |3 - 4|12n + |3 - 8|(36n^2 - 12n) + |4 - 8|12n + |8 - 8|(18n^2 - 12n) \\ &= 180n^2 - 12n, \end{aligned}$$

$$\text{IR1}(\sigma_n) = F(\sigma_n) - \left(\frac{2p}{q}\right)M_1(\sigma_n) = (5580n^2 - 1152n) - \frac{2(90n^2)}{45n^2 - 3n} [900n^2 - 96n]$$

$$= -3600n^6 + 384n^5 + 2700n^3 + 5292n^2 - 1152n,$$

$$\text{IR2}(\sigma_n) = \sqrt{\frac{M_2(\sigma_n)}{p}} - \left(\frac{2p}{q}\right) = \sqrt{\frac{2340n^2 - 528n}{90n^2}} - \left(\frac{2(90n^2)}{45n^2 - 3n}\right) = \sqrt{\frac{2}{15}}\sqrt{n^3(195n - 44)} + \frac{60n}{1 - 15n},$$

$$\text{IRF}(\sigma_n) = F(\sigma_n) - 2M_2(\sigma_n) = (5580n^2 - 1152n) - 2(2340n^2 - 528n) = 900n^2 - 96n,$$

$$\text{IRFW}(\sigma_n) = \frac{\text{IRF}(\sigma_n)}{M_2(\sigma_n)} = \frac{900n^2 - 96n}{2340n^2 - 528n},$$

$$\begin{aligned} \text{IRA}(\sigma_n) &= \sum_{lm \in X(\sigma)} \left( (\mathfrak{F}(l))^{-1/2} - (\mathfrak{F}(m))^{-1/2} \right)^2 = \left( \frac{1}{\sqrt{3}} - \frac{1}{\sqrt{3}} \right)^2 (36n^2) + \left( \frac{1}{\sqrt{3}} - \frac{1}{\sqrt{4}} \right)^2 (12n) \\ &\quad + \left( \frac{1}{\sqrt{3}} - \frac{1}{\sqrt{8}} \right)^2 (36n^2 - 12n) + \left( \frac{1}{\sqrt{4}} - \frac{1}{\sqrt{8}} \right)^2 (12n) + \left( \frac{1}{\sqrt{8}} - \frac{1}{\sqrt{8}} \right)^2 (18n^2 - 12n) \\ &= 1.8030n^2 - 0.2718n, \end{aligned}$$

$$\begin{aligned} \text{IRB}(\sigma_n) &= \sum_{lm \in X(\sigma)} \left( (\mathfrak{F}(l))^{1/2} - (\mathfrak{F}(m))^{1/2} \right)^2 = (\sqrt{3} - \sqrt{4})^2 (12n) + (\sqrt{3} - \sqrt{8})^2 (36n^2 - 12n) + (\sqrt{4} - \sqrt{8})^2 (12n) \\ &= 43.2734n^2 - 5.3274n, \end{aligned}$$

$$\begin{aligned} \text{IRC}(\sigma_n) &= \sum_{lm \in X(\sigma)} \frac{\sqrt{\mathfrak{F}(l)\mathfrak{F}(m)}}{p} - \frac{2p}{q} \\ &= \frac{\sqrt{9}(36n^2) + \sqrt{12}(12n) + \sqrt{24}(36n^2 - 12n) + \sqrt{32}(12n) + \sqrt{64}(18n^2 - 12n)}{90n^2} - \left( \frac{2(90n^2)}{45n^2 - 3n} \right) \\ &= \frac{428.36n - 45.345}{90n} - \frac{60n}{15n - 1}, \end{aligned}$$

$$\begin{aligned} \text{IRDIF}(\sigma_n) &= \sum_{lm \in X(\sigma)} \left| \frac{\mathfrak{F}(l)}{\mathfrak{F}(m)} - \frac{\mathfrak{F}(m)}{\mathfrak{F}(l)} \right| \\ &= \left| \frac{3}{3} - \frac{3}{3} \right| 36n^2 + \left| \frac{3}{4} - \frac{4}{3} \right| 12n + \left| \frac{3}{8} - \frac{8}{3} \right| (36n^2 - 12n) + \left| \frac{4}{8} - \frac{8}{4} \right| 12n + \left| \frac{8}{8} - \frac{8}{8} \right| (18n^2 - 12n) \\ &= 82.5n^2 - 2.5n, \end{aligned}$$

$$\begin{aligned} \text{IRL}(\sigma_n) &= \sum_{lm \in X(\sigma)} |\ln \mathfrak{F}(l) - \ln \mathfrak{F}(m)| \\ &= 36n^2 |\ln 3 - \ln 3| + 12n |\ln 3 - \ln 4| + (36n^2 - 12n) |\ln 3 - \ln 8| + (12n) |\ln 4 - \ln 8| + (18n^2 - 12n) |\ln 8 - \ln 8| \\ &= 35.3088n^2 - 0.0012n, \end{aligned}$$

$$\begin{aligned} \text{IRLU}(\sigma_n) &= \sum_{lm \in X(\sigma)} \frac{|\mathfrak{F}(l) - \mathfrak{F}(m)|}{\min(\mathfrak{F}(l), \mathfrak{F}(m))} \\ &= \frac{|3 - 3|}{\min(3, 3)} (36n^2) + \frac{|3 - 4|}{\min(3, 4)} (12n) + \frac{|3 - 8|}{\min(3, 8)} (36n^2 - 12n) + \frac{|4 - 8|}{\min(4, 8)} (12n) + \frac{|8 - 8|}{\min(8, 8)} (18n^2 - 12n) \\ &= 4n + 60n^2 - 20n + 12n \\ &= 4n(15n - 1), \end{aligned}$$

$$\begin{aligned}
\text{IRLF}(\sigma_n) &= \sum_{lm \in X(\sigma)} \frac{|\mathfrak{F}(l) - \mathfrak{F}(m)|}{\sqrt{\mathfrak{F}(l)\mathfrak{F}(m)}} \\
&= 36n^2 \left( \frac{|3-3|}{\sqrt{9}} \right) + 12n \left( \frac{|3-4|}{\sqrt{12}} \right) + (36n^2 - 12n) \left( \frac{|3-8|}{\sqrt{24}} \right) + 12n \left( \frac{|4-8|}{\sqrt{32}} \right) + (18n^2 - 12n) \left( \frac{|8-8|}{\sqrt{64}} \right) \\
&= \sqrt{12}n + 36.74n^2 - 12.247n + 8.4852n \\
&= 36.74n^2 - 0.29769n, \\
\text{IRLA}(\sigma_n) &= 2 \sum_{lm \in X(\sigma)} \frac{|\mathfrak{F}(l) - \mathfrak{F}(m)|}{\mathfrak{F}(l) + \mathfrak{F}(m)} \\
&= 2(36n^2) \left( \frac{|3-3|}{3+3} \right) + 2(12n) \left( \frac{|3-4|}{3+4} \right) + 2(36n^2 - 12n) \left( \frac{|3-8|}{3+8} \right) + 2(12n) \left( \frac{|4-8|}{4+8} \right) + 2(18n^2 - 12n) \left( \frac{|8-8|}{8+8} \right) \\
&= 32.7272n^2 + 0.5195n, \\
\text{IRGA}(\sigma_n) &= \sum_{lm \in X(\sigma)} \ln \frac{\mathfrak{F}(l) + \mathfrak{F}(m)}{2\sqrt{\mathfrak{F}(l)\mathfrak{F}(m)}} \\
&= 36n^2 \left( \ln \frac{6}{2\sqrt{9}} \right) + 12n \left( \ln \frac{7}{2\sqrt{12}} \right) + (36n^2 - 12n) \left( \ln \frac{11}{2\sqrt{24}} \right) + 12n \left( \ln \frac{12}{2\sqrt{32}} \right) + (18n^2 - 12n) \left( \ln \frac{16}{2\sqrt{64}} \right) \\
&= 4.16592n^2 - 0.55824n.
\end{aligned} \tag{4}$$

The structure of Benzenoid dominating planar octahedron is constructed and the topological properties of this structure is well explained [33]. The 2-dimensional structure of Benzenoid dominating planar octahedron structure is given in Figure 2. We denote the graph of Benzenoid dominating planar octahedron by  $\nu_n$ ,  $n \geq 2$ , where  $n$  denotes the dimension of Benzenoid dominating planar octahedron. Figure 2 depicts the 2-dimensional structure of the molecular graph of  $\nu_2$ . The total number of vertices ( $t$ ) and edges ( $s$ ) in the structure of Benzenoid dominating planar octahedron are  $27n^2 - 33n + 12$  and  $270n^2 - 378n + 156$ .

The set of edges of Benzenoid dominating planar octahedron structure is divided into five partitions based on the degree of end vertices. The first partition of edge includes

of  $108n^2 - 132n + 48$  edges  $lm$ , where  $\mathfrak{F}(l) = 3$  and  $\mathfrak{F}(m) = 3$ . The second partition of edge includes of  $24n - 12$  edges  $lm$ , where  $\mathfrak{F}(l) = 3$  and  $\mathfrak{F}(m) = 4$ . The third partition of edge includes of  $108n^2 - 132n + 48$  edges  $lm$ , where  $\mathfrak{F}(l) = 3$  and  $\mathfrak{F}(m) = 8$ . The fourth partition of edge includes of  $24n - 12$  edges  $lm$ , where  $\mathfrak{F}(l) = 4$  and  $\mathfrak{F}(m) = 8$ . The fifth partition of edge includes of  $54n^2 - 162n + 84$  edges  $lm$ , where  $\mathfrak{F}(l) = 8$  and  $\mathfrak{F}(m) = 8$ . Table 2 shows the edge partition of Benzenoid dominating planar octahedron structure.  $\square$

**Theorem 2.** Consider the graph  $\nu_n$ ,  $n \geq 2$ , then the irregularity indices of Benzenoid dominating planar octahedron structure are

$$\text{VAR}(\nu_n) = \frac{2700n^2 - 4380n + 1932}{27n^2 - 33n + 12} - \left( \frac{2(270n^2 - 378n + 156)}{27n^2 - 33n + 12} \right)^2,$$

$$AL(\nu_n) = 540n^2 - 540n + 180,$$

$$\text{IR1}(\nu_n) = (16740n^2 - 19044n + 6732) - \frac{2(270n^2 - 378n + 156)}{27n^2 - 33n + 12} [2700n^2 - 4380n + 1932],$$

$$\text{IR2}(\nu_n) = \sqrt{\frac{7020n^2 - 13668n + 6432}{270n^2 - 378n + 156}} - \left( \frac{2(270n^2 - 378n + 156)}{27n^2 - 33n + 12} \right),$$

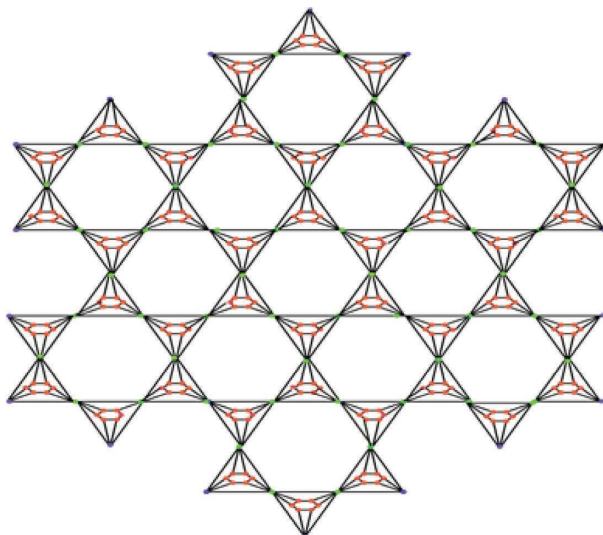


FIGURE 2: Benzenoid dominating planar octahedron structure of dimension 2.

TABLE 2: Edge partition of benzenoid dominating planar octahedron structure.

$(\mathfrak{I}(l), \mathfrak{I}(m))$	(3, 3)	(3, 4)	(3, 8)	(4, 8)	(8, 8)
Number of edges	$108n^2 - 132n + 48$	$24n - 12$	$108n^2 - 132n + 48$	$24n - 12$	$54n^2 - 162n + 84$

$$\text{IRF}(\nu_n) = 2700n^2 + 8292n - 6132,$$

$$\text{IRFW}(\nu_n) = \frac{2700n^2 + 8292n - 6132}{7020n^2 - 13668n + 6432},$$

$$\text{IRA}(\nu_n) = 5.40692n^2 - 5.95031n + 2.074,$$

$$\text{IRB}(\nu_n) = 129.82n^2 - 140.4752n + 48.6009,$$

$$\text{IRC}(\nu_n) = \frac{1285.08n^2 - 2119.636n + 941.651}{270n^2 - 378n + 156} - \left( \frac{2(270n^2 - 378n + 156)}{27n^2 - 33n + 12} \right), \quad (5)$$

$$\text{IRDIF}(\nu_n) = -247.5n^2 + 252.5n - 85,$$

$$\text{IRL}(\nu_n) = -105.926n^2 - 23.53776n + 87.25368,$$

$$\text{IRLU}(\nu_n) = 180n^2 - 188n + 64,$$

$$\text{IRLF}(\nu_n) = 110.22n^2 - 110.82n + 37.0403,$$

$$\text{IRLA}(\nu_n) = 98.1818n^2 - 97.1429n + 32.2078,$$

$$\text{IRGA}(\nu_n) = 12.4977n^2 - 15.0278n + 4.72428.$$

*Proof.* Applying the partition of edge based on degrees of end vertices of each edge of the Benzenoid dominating planar octahedron structure  $\nu_n$  depicted in Table 2, we

compute the irregularity indices of the Benzenoid dominating planar octahedron structure  $\nu_n$ , and the mathematical calculations are given as follows:

$$\text{VAR}(\nu_n) = \frac{M_1(\nu_n)}{t} - \left(\frac{2s}{t}\right)^2 = \frac{2700n^2 - 4380n + 1932}{27n^2 - 33n + 12} - \left(\frac{2(270n^2 - 378n + 156)}{27n^2 - 33n + 12}\right)^2,$$

$$\begin{aligned} \text{AL}(\nu_n) &= \sum_{lm \in X(\nu)} |\mathfrak{F}(l) - \mathfrak{F}(m)| = |3 - 3|(108n^2 - 132n + 48) + |3 - 4|(24n - 12) + |3 - 8|(108n^2 - 132n + 48) \\ &\quad + |4 - 8|(24n - 12) + |8 - 8|(54n^2 - 162n + 84) \\ &= 540n^2 - 540n + 180, \end{aligned}$$

$$\text{IR1}(\nu_n) = F(\nu_n) - \left(\frac{2s}{t}\right)M_1(\nu_n) = (16740n^2 - 19044n + 6732) - \frac{2(270n^2 - 378n + 156)}{27n^2 - 33n + 12} [2700n^2 - 4380n + 1932],$$

$$\text{IR2}(\nu_n) = \sqrt{\frac{M_2(\nu_n)}{s}} - \left(\frac{2s}{t}\right) = \sqrt{\frac{7020n^2 - 13668n + 6432}{270n^2 - 378n + 156}} - \left(\frac{2(270n^2 - 378n + 156)}{27n^2 - 33n + 12}\right),$$

$$\begin{aligned} \text{IRF}(\nu_n) &= F(\nu_n) - 2M_2(\nu_n) = (16740n^2 - 19044n + 6732) - 2(7020n^2 - 13668n + 6432) \\ &= 2700n^2 + 8292n - 6132, \end{aligned}$$

$$\text{IRFW}(\nu_n) = \frac{\text{IRF}(\nu_n)}{M_2(\nu_n)} = \frac{2700n^2 + 8292n - 6132}{7020n^2 - 13668n + 6432},$$

$$\begin{aligned} \text{IRA}(\nu_n) &= \sum_{lm \in X(\nu)} \left( (\mathfrak{F}(l))^{-1/2} - (\mathfrak{F}(m))^{-1/2} \right)^2 = \left( \frac{1}{\sqrt{3}} - \frac{1}{\sqrt{3}} \right)^2 (108n^2 - 132n + 48) + \left( \frac{1}{\sqrt{3}} - \frac{1}{\sqrt{4}} \right)^2 (24n - 12) \\ &\quad + \left( \frac{1}{\sqrt{3}} - \frac{1}{\sqrt{8}} \right)^2 (108n^2 - 132n + 48) + \left( \frac{1}{\sqrt{4}} - \frac{1}{\sqrt{8}} \right)^2 (24n - 12) + \left( \frac{1}{\sqrt{8}} - \frac{1}{\sqrt{8}} \right)^2 (54n^2 - 162n + 84) \\ &= 5.40692n^2 - 5.95031n + 2.074, \end{aligned}$$

$$\begin{aligned} \text{IRB}(\nu_n) &= \sum_{lm \in X(\nu)} \left( (\mathfrak{F}(l))^{1/2} - (\mathfrak{F}(m))^{1/2} \right)^2 = (\sqrt{3} - \sqrt{4})^2 (24n - 12) \\ &\quad + (\sqrt{3} - \sqrt{8})^2 (108n^2 - 132n + 48) + (\sqrt{4} - \sqrt{8})^2 (24n - 12) \\ &= 129.82n^2 - 140.4752n + 48.6009, \end{aligned}$$

$$\begin{aligned} \text{IRC}(\nu_n) &= \sum_{lm \in X(\nu)} \frac{\sqrt{\mathfrak{F}(l)\mathfrak{F}(m)}}{s} - \frac{2s}{t} \\ &= \frac{\sqrt{9}(108n^2 - 132n + 48) + \sqrt{12}(24n - 12) + \sqrt{24}(108n^2 - 132n + 48) + \sqrt{32}(24n - 12) + \sqrt{64}(54n^2 - 162n + 84)}{270n^2 - 378n + 156} \\ &\quad - \left( \frac{2(270n^2 - 378n + 156)}{27n^2 - 33n + 12} \right) \\ &= \frac{1285.08n^2 - 2119.636n + 941.651}{270n^2 - 378n + 156} - \left( \frac{2(270n^2 - 378n + 156)}{27n^2 - 33n + 12} \right), \end{aligned}$$

$$\text{IRDIF}(\nu_n) = \sum_{lm \in X(\nu)} \left| \frac{\mathfrak{F}(l)}{\mathfrak{F}(m)} - \frac{\mathfrak{F}(m)}{\mathfrak{F}(l)} \right|,$$

$$\begin{aligned}
&= \left| \frac{3}{3} - \frac{3}{3} \right| (108n^2 - 132n + 48) + \left| \frac{3}{4} - \frac{4}{3} \right| (24n - 12) + \left| \frac{3}{8} - \frac{8}{3} \right| (108n^2 - 132n + 48) + \left| \frac{4}{8} - \frac{8}{4} \right| (24n - 12) \\
&\quad + \left| \frac{8}{8} - \frac{8}{8} \right| (54n^2 - 162n + 84) \\
&= -247.5n^2 + 252.5n - 85,
\end{aligned}$$

$$\begin{aligned}
\text{IRL}(v_n) &= \sum_{lm \in X(v)} |\ln \mathfrak{F}(l) - \ln \mathfrak{F}(m)| \\
&= (108n^2 - 132n + 48)|\ln 3 - \ln 3| + (24n - 12)|\ln 3 - \ln 4| + (108n^2 - 132n + 48)|\ln 3 - \ln 8| \\
&\quad + (24n - 12)|\ln 4 - \ln 8| + (54n^2 - 162n + 84)|\ln 8 - \ln 8| \\
&= -105.926n^2 - 23.53776n + 87.25368,
\end{aligned}$$

$$\begin{aligned}
\text{IRLU}(v_n) &= \sum_{lm \in X(v)} \frac{|\mathfrak{F}(l) - \mathfrak{F}(m)|}{\min(\mathfrak{F}(l), \mathfrak{F}(m))} \\
&= \frac{|3-3|}{\min(3,3)}(108n^2 - 132n + 48) + \frac{|3-4|}{\min(3,4)}(24n - 12) + \frac{|3-8|}{\min(3,8)}(108n^2 - 132n + 48) \\
&\quad + \frac{|4-8|}{\min(4,8)}(24n - 12) + \frac{|8-8|}{\min(8,8)}(54n^2 - 162n + 84) \\
&= 180n^2 - 188n + 64,
\end{aligned}$$

$$\begin{aligned}
\text{IRLF}(v_n) &= \sum_{lm \in X(v)} \frac{|\mathfrak{F}(l) - \mathfrak{F}(m)|}{\sqrt{\mathfrak{F}(l)\mathfrak{F}(m)}} \\
&= (108n^2 - 132n + 48) \left( \frac{|3-3|}{\sqrt{9}} \right) + (24n - 12) \left( \frac{|3-4|}{\sqrt{12}} \right) + (108n^2 - 132n + 48) \left( \frac{|3-8|}{\sqrt{24}} \right) \\
&\quad + (24n - 12) \left( \frac{|4-8|}{\sqrt{32}} \right) + (54n^2 - 162n + 84) \left( \frac{|8-8|}{\sqrt{64}} \right) \\
&= 110.22n^2 - 110.82n + 37.0403,
\end{aligned}$$

$$\begin{aligned}
\text{IRLA}(v_n) &= 2 \sum_{lm \in X(v)} \frac{|\mathfrak{F}(l) - \mathfrak{F}(m)|}{\mathfrak{F}(l) + \mathfrak{F}(m)} \\
&= 2(108n^2 - 132n + 48) \left( \frac{|3-3|}{3+3} \right) + 2(24n - 12) \left( \frac{|3-4|}{3+4} \right) + 2(108n^2 - 132n + 48) \left( \frac{|3-8|}{3+8} \right) \\
&\quad + 2(24n - 12) \left( \frac{|4-8|}{4+8} \right) + 2(54n^2 - 162n + 84) \left( \frac{|8-8|}{8+8} \right) \\
&= 98.1818n^2 - 97.1429n + 32.2078,
\end{aligned}$$



$$\begin{aligned}
\text{IRGA}(\gamma_n) &= \sum_{lm \in X(\gamma)} \ln \frac{\mathfrak{F}(l) + \mathfrak{F}(m)}{2\sqrt{\mathfrak{F}(l)\mathfrak{F}(m)}} \\
&= (108n^2 - 132n + 48) \left( \ln \frac{6}{2\sqrt{9}} \right) + (24n - 12) \left( \ln \frac{7}{2\sqrt{12}} \right) + (108n^2 - 132n + 48) \left( \ln \frac{11}{2\sqrt{24}} \right) \\
&\quad + (24n - 12) \left( \ln \frac{12}{2\sqrt{32}} \right) + (54n^2 - 162n + 84) \left( \ln \frac{16}{2\sqrt{64}} \right) \\
&= 12.4977n^2 - 15.0278n + 4.72428.
\end{aligned} \tag{6}$$

The structure of Benzenoid hex planar octahedron is constructed and the topological properties of this structure are well discussed [33]. The 2-dimensional structure of Benzenoid hex planar octahedron structure is given in Figure 3. We represent the graph of Benzenoid hex planar octahedron by  $\mu_n$ ,  $n \geq 2$ , where  $n$  denotes the dimension of Benzenoid hex planar octahedron. Figure 3 depicts the 2-dimensional structure of the molecular graph of  $\mu_2$ . The total number of vertices ( $u$ ) and edges ( $v$ ) in the structure of Benzenoid hex planar octahedron are  $45n^2 + 51n + 6$  and  $90n^2 + 24n + 6$ .

The set of edges of Benzenoid hex planar octahedron structure is divided into five partitions based on the degree of end vertices. The first partition of edge includes of 12 edges  $lm$ , where  $\mathfrak{F}(l) = 2$  and  $\mathfrak{F}(m) = 5$ . The second partition of

edge includes of  $36n^2 - 36n$  edges  $lm$ , where  $\mathfrak{F}(l) = 3$  and  $\mathfrak{F}(m) = 3$ . The third partition of edge includes of  $24n$  edges  $lm$ , where  $\mathfrak{F}(l) = 3$  and  $\mathfrak{F}(m) = 5$ . The fourth partition of edge includes of  $36n^2 + 12n$  edges  $lm$ , where  $\mathfrak{F}(l) = 3$  and  $\mathfrak{F}(m) = 8$ . The fifth partition of edge includes of  $12n - 6$  edges  $lm$ , where  $\mathfrak{F}(l) = 5$  and  $\mathfrak{F}(m) = 5$ . The sixth partition of edge includes of  $12n$  edges  $lm$ , where  $\mathfrak{F}(l) = 5$  and  $\mathfrak{F}(m) = 8$ . The seventh partition of edge includes of  $18n^2$  edges  $lm$ , where  $\mathfrak{F}(l) = 8$  and  $\mathfrak{F}(m) = 8$ . Table 3 shows the edge partition of Benzenoid hex planar octahedron structure.  $\square$

**Theorem 3.** Consider the graph  $\mu_n$ ,  $n \geq 2$ , then the irregularity indices of Benzenoid hex planar octahedron structure are

$$\begin{aligned}
\text{VAR}(\mu_n) &= \frac{900n^2 - 384n + 24}{45n^2 + 51n + 6} - \left( \frac{180n^2 + 48n + 12}{45n^2 + 51n + 6} \right)^2, \\
AL(\mu_n) &= 180n^2 + 144n + 36, \\
\text{IR1}(\mu_n) &= \frac{413100n^4 + 490860n^3 + 243360n^2 + 29952n}{45n^2 + 51n + 6}, \\
\text{IR2}(\mu_n) &= \sqrt{\frac{2340n^2 + 1104n - 30}{90n^2 + 24n + 6}} - \left( \frac{180n^2 + 48n + 12}{45n^2 + 51n + 6} \right), \\
\text{IRF}(\mu_n) &= 900n^2 + 1800n + 108, \\
\text{IRFW}(\mu_n) &= \frac{900n^2 + 1800n + 108}{2340n^2 + 1104n - 30}, \\
\text{IRA}(\mu_n) &= 1.80311184n^2 + 1.11276567n + 0.810495, \\
\text{IRB}(\mu_n) &= 43.2734n^2 + 24.7318n + 8.10533616, \\
\text{IRC}(\mu_n) &= \frac{428.3632n^2 - 179.63401n + 7.94733}{90n^2 + 24n + 6} - \left( \frac{180n^2 + 48n + 12}{45n^2 + 51n + 6} \right), \\
\text{IRDIF}(\mu_n) &= 82.49976n^2 + 64.783n + 25.2,
\end{aligned}$$

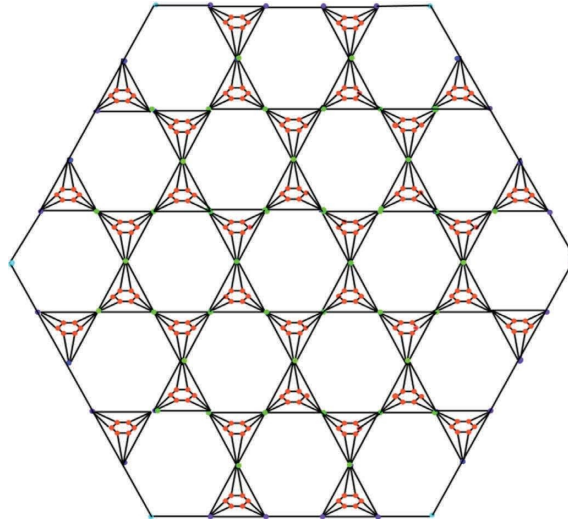


FIGURE 3: Benzenoid hex planar octahedron structure of dimension 2.

TABLE 3: Edge partition of benzenoid hex planar octahedron structure.

$(\mathfrak{I}(l), \mathfrak{I}(m))$	(2, 5)	(3, 3)	(3, 5)	(3, 8)	(5, 5)	(5, 8)	(8, 8)
Number of edges	12	$36n^2 - 36n$	$24n$	$36n^2 + 12n$	$12n - 6$	$12n$	$18n^2$

$$\text{IRL}(\mu_n) = 73.7612n^2 + 84.72643n + 18.62010,$$

$$\text{IRLU}(\mu_n) = 60n^2 + 43.2n + 18,$$

$$\text{IRLF}(\mu_n) = 36.74234n^2 + 30.3329867n + 11.3841996, \quad (7)$$

$$\text{IRLA}(\mu_n) = 32.7272n^2 + 28.44746n + 10.2857,$$

$$\text{IRGA}(\mu_n) = 118.5759n^2 + 84.894662n + 28.8486661.$$

*Proof.* Applying the partition of edge based on degrees of end vertices of each edge of the Benzenoid hex planar octahedron structure  $\mu_n$  depicted in Table 3, we compute the

irregularity indices of the Benzenoid hex planar octahedron structure  $\mu_n$  and the mathematical calculations are given as follows:

$$\text{VAR}(\mu_n) = \frac{M_1(\mu_n)}{u} - \left(\frac{2v}{u}\right)^2 = \frac{900n^2 - 384n + 24}{45n^2 + 51n + 6} - \left(\frac{180n^2 + 48n + 12}{45n^2 + 51n + 6}\right)^2,$$

$$\text{AL}(\mu_n) = \sum_{lm \in X(\mu)} |\mathfrak{I}(l) - \mathfrak{I}(m)| = |2 - 5|(12) + |3 - 3|(36n^2 - 36n) + |3 - 5|(24n) + |3 - 8|(36n^2 + 12n)$$

$$+ |5 - 5|(12n - 6) + |5 - 8|(12n) + |8 - 8|(18n^2)$$

$$= 180n^2 + 144n + 36,$$

$$\begin{aligned} \text{IR1}(\mu_n) &= F(\mu_n) - \left(\frac{2v}{u}\right)M_1(\mu_n) = (5580n^2 + 4008n + 48) - \left(\frac{180n^2 + 48n + 12}{45n^2 + 51n + 6}\right)[900n^2 - 384n + 24] \\ &= \frac{413100n^4 + 490860n^3 + 243360n^2 + 29952n}{45n^2 + 51n + 6}, \end{aligned}$$

$$\text{IR2}(\mu_n) = \sqrt{\frac{M_2(\mu_n)}{v}} - \left(\frac{2v}{u}\right) = \sqrt{\frac{2340n^2 + 1104n - 30}{90n^2 + 24n + 6}} - \left(\frac{180n^2 + 48n + 12}{45n^2 + 51n + 6}\right),$$

$$\begin{aligned} \text{IRF}(\mu_n) &= F(\mu_n) - 2M_2(\mu_n) = (5580n^2 + 4008n + 48) - 2(2340n^2 + 1104n - 30) \\ &= 900n^2 + 1800n + 108, \end{aligned}$$

$$\begin{aligned} \text{IRFW}(\mu_n) &= \frac{\text{IRF}(\mu_n)}{M_2(\mu_n)} \\ &= \frac{900n^2 + 1800n + 108}{2340n^2 + 1104n - 30} \end{aligned}$$

$$\begin{aligned} \text{IRA}(\mu_n) &= \sum_{lm \in X(\mu)} \left( (\mathfrak{F}(l))^{-1/2} - (\mathfrak{F}(m))^{-1/2} \right)^2 = \left(\frac{1}{\sqrt{2}} - \frac{1}{\sqrt{5}}\right)^2 (12) + \left(\frac{1}{\sqrt{3}} - \frac{1}{\sqrt{3}}\right)^2 (36n^2 - 36n) + \left(\frac{1}{\sqrt{3}} - \frac{1}{\sqrt{5}}\right)^2 (24n) \\ &\quad + \left(\frac{1}{\sqrt{3}} - \frac{1}{\sqrt{8}}\right)^2 (36n^2 + 12n) + \left(\frac{1}{\sqrt{5}} - \frac{1}{\sqrt{5}}\right)^2 (12n - 6) + \left(\frac{1}{\sqrt{5}} - \frac{1}{\sqrt{8}}\right)^2 (12n) + \left(\frac{1}{\sqrt{8}} - \frac{1}{\sqrt{8}}\right)^2 (18n^2) \\ &= 1.80311184n^2 + 1.11276567n + 0.810495, \end{aligned}$$

$$\begin{aligned} \text{IRB}(\mu_n) &= \sum_{lm \in X(\mu)} \left( (\mathfrak{F}(l))^{1/2} - (\mathfrak{F}(m))^{1/2} \right)^2 = (\sqrt{2} - \sqrt{5})^2 (12) + (\sqrt{3} - \sqrt{3})^2 (36n^2 - 36n) + (\sqrt{3} - \sqrt{5})^2 (24n) \\ &\quad + (\sqrt{3} - \sqrt{8})^2 (36n^2 + 12n) + (\sqrt{5} - \sqrt{5})^2 (12n - 6) + (\sqrt{5} - \sqrt{8})^2 (12n) + (\sqrt{8} - \sqrt{8})^2 (18n^2) \\ &= 43.2734n^2 + 24.7318n + 8.10533616, \end{aligned}$$

$$\begin{aligned} \text{IRC}(\mu_n) &= \sum_{lm \in X(\mu)} \frac{\sqrt{\mathfrak{F}(l)\mathfrak{F}(m)}}{v} - \frac{2v}{u} \\ &= \frac{\sqrt{10}(12) + \sqrt{9}(36n^2 - 36n) + \sqrt{15}(24n) + \sqrt{24}(36n^2 + 12n) + \sqrt{25}(12n - 6) + \sqrt{40}(12n) + \sqrt{64}(18n^2)}{90n^2 + 24n + 6} \\ &\quad - \left(\frac{180n^2 + 48n + 12}{45n^2 + 51n + 6}\right) \\ &= \frac{428.3632n^2 - 179.63401n + 7.94733}{90n^2 + 24n + 6} - \left(\frac{180n^2 + 48n + 12}{45n^2 + 51n + 6}\right), \end{aligned}$$

$$\text{IRDIF}(\mu_n) = \sum_{lm \in X(\mu)} \left| \frac{\mathfrak{F}(l)}{\mathfrak{F}(m)} - \frac{\mathfrak{F}(m)}{\mathfrak{F}(l)} \right|$$

$$\begin{aligned}
&= \left| \frac{2}{5} - \frac{5}{2} \right| (12) + \left| \frac{3}{3} - \frac{3}{3} \right| (36n^2 - 36n) + \left| \frac{3}{5} - \frac{5}{3} \right| (24n) + \left| \frac{3}{8} - \frac{8}{3} \right| (36n^2 + 12n) + \left| \frac{5}{5} - \frac{5}{5} \right| (12n - 6) \\
&\quad + \left| \frac{5}{8} - \frac{8}{5} \right| (12n) + \left| \frac{8}{8} - \frac{8}{8} \right| (18n^2) \\
&= 82.49976n^2 + 64.783n + 25.2,
\end{aligned}$$

$$\begin{aligned}
\text{IRL}(\mu_n) &= \sum_{lm \in X(\mu)} |\ln \mathfrak{F}(l) - \ln \mathfrak{F}(m)|, \\
&= (12)|\ln 2 - \ln 5| + (36n^2 - 36n)|\ln 3 - \ln 3| + (24n)|\ln 3 - \ln 5| + (36n^2 + 12n)|\ln 3 - \ln 8| \\
&\quad + (12n - 6)|\ln 5 - \ln 5| + (12n)|\ln 5 - \ln 8| + (18n^2)|\ln 8 - \ln 8| \\
&= 73.7612n^2 + 84.72643n + 18.62010,
\end{aligned}$$

$$\begin{aligned}
\text{IRLU}(\mu_n) &= \sum_{lm \in X(\mu)} \frac{|\mathfrak{F}(l) - \mathfrak{F}(m)|}{\min(\mathfrak{F}(l), \mathfrak{F}(m))} \\
&= \frac{|2 - 5|}{\min(2, 5)} (12) + \frac{|3 - 3|}{\min(3, 3)} (36n^2 - 36n) + \frac{|3 - 5|}{\min(3, 5)} (24n) + \frac{|3 - 8|}{\min(3, 8)} (36n^2 + 12n) + \frac{|5 - 5|}{\min(5, 5)} (12n - 6) \\
&\quad + \frac{|5 - 8|}{\min(5, 8)} (12n) + \frac{|8 - 8|}{\min(8, 8)} (18n^2) \\
&= 60n^2 + 43.2n + 18,
\end{aligned}$$

$$\begin{aligned}
\text{IRLF}(\mu_n) &= \sum_{lm \in X(\mu)} \frac{|\mathfrak{F}(l) - \mathfrak{F}(m)|}{\sqrt{\mathfrak{F}(l)\mathfrak{F}(m)}} \\
&= (12) \left( \frac{|2 - 5|}{\sqrt{10}} \right) + (36n^2 - 36n) \left( \frac{|3 - 3|}{\sqrt{9}} \right) + (24n) \left( \frac{|3 - 5|}{\sqrt{15}} \right) + (36n^2 + 12n) \left( \frac{|3 - 8|}{\sqrt{24}} \right) + (12n - 6) \left( \frac{|5 - 5|}{\sqrt{25}} \right) \\
&\quad + (12n) \left( \frac{|5 - 8|}{\sqrt{40}} \right) + (18n^2) \left( \frac{|8 - 8|}{\sqrt{64}} \right) \\
&= 36.74234n^2 + 30.3329867n + 11.3841996,
\end{aligned}$$

$$\begin{aligned}
\text{IRLA}(\mu_n) &= 2 \sum_{lm \in X(\mu)} \frac{|\mathfrak{F}(l) - \mathfrak{F}(m)|}{\mathfrak{F}(l) + \mathfrak{F}(m)} \\
&= 2(12) \left( \frac{|2 - 5|}{2 + 5} \right) + 2(36n^2 - 36n) \left( \frac{|3 - 3|}{3 + 3} \right) + 2(24n) \left( \frac{|3 - 5|}{3 + 5} \right) + 2(36n^2 + 12n) \left( \frac{|3 - 8|}{3 + 8} \right) + 2(12n - 6) \left( \frac{|5 - 5|}{5 + 5} \right) \\
&\quad + 2(12n) \left( \frac{|5 - 8|}{5 + 8} \right) + 2(18n^2) \left( \frac{|8 - 8|}{8 + 8} \right) \\
&= 32.7272n^2 + 28.44746n + 10.2857,
\end{aligned}$$

TABLE 4: Numerical values of irregularity indices for  $\sigma_n$ .

Irregularity indices	$n = 1$	$n = 2$	$n = 3$	$n = 4$	$n = 5$
VAR ( $\sigma_n$ )	0.7755	2.4637	2.9917	3.2496	3.4024
AL ( $\sigma_n$ )	168	696	1584	2832	4440
IR1 ( $\sigma_n$ )	3624	-17764	-2414016	-14099520	-54585960
IR2 ( $\sigma_n$ )	0.2013	15.073	40.0407	75.1820	120.5118
IRF ( $\sigma_n$ )	804	3408	7812	14016	22020
IRFW ( $\sigma_n$ )	0.44370	0.41040	0.40110	0.39673	0.39419
IRA ( $\sigma_n$ )	1.5312	6.6684	15.4116	27.7608	43.716
IRB ( $\sigma_n$ )	37.946	162.4388	373.4784	671.0648	1055.198
IRC ( $\sigma_n$ )	-0.29992	0.36970	0.50070	0.56580	0.6047
IRDIF ( $\sigma_n$ )	80	325	735	1310	2050
IRL ( $\sigma_n$ )	35.3076	141.2328	317.7756	564.93	882.714
IRLU ( $\sigma_n$ )	56	232	528	944	1480
IRLF ( $\sigma_n$ )	36.44231	146.364	329.766	586.6492	917.01155
IRLA ( $\sigma_n$ )	33.2467	131.9478	296.1033	525.7132	820.7775
IRGA ( $\sigma_n$ )	3.60768	15.5472	35.81856	64.4217	101.3568

TABLE 5: Numerical values of irregularity indices for  $\nu_n$ .

Irregularity indices	$n = 1$	$n = 2$	$n = 3$	$n = 4$	$n = 5$
VAR ( $\nu_n$ )	-214	-242.49	-262.60	-272.5	-278.28
AL ( $\nu_n$ )	180	1260	3420	6660	10980
IR1 ( $\nu_n$ )	396	-35009.3	-143453	-326232	-583477
IR2 ( $\nu_n$ )	-16 + 2.12	-13.9112	-14.1766	-14.35032	-14.4596
IRF ( $\nu_n$ )	4860	21252	43044	70236	102828
IRFW ( $\nu_n$ )	-22.5	2.9615	1.5046	1.0960	0.9052
IRA ( $\nu_n$ )	1.53061	11.80106	32.885	64.783	107.495
IRB ( $\nu_n$ )	37.9457	286.9305	795.5553	1563.8201	2591.7249
IRC ( $\nu_n$ )	-13.76885	-13.9388	-14.38090	-14.6058	-14.7386
IRDIF ( $\nu_n$ )	-80	-570	-1555	-3035	-5010
IRL ( $\nu_n$ )	-42.21002	-383.525	-936.693	-1701.713	-2678.58
IRLU ( $\nu_n$ )	56	408	1120	2192	3624
IRLF ( $\nu_n$ )	36.4403	256.2803	696.5603	1357.2803	2238.4403
IRLA ( $\nu_n$ )	33.246	230.6492	624.41	1214.545	2001.0383
IRGA ( $\nu_n$ )	2.19418	24.6594	72.12018	144.576	242.027

TABLE 6: Numerical values of irregularity indices for  $\mu_n$ .

Irregularity indices	$n = 1$	$n = 2$	$n = 3$	$n = 4$	$n = 5$
VAR ( $\mu_n$ )	-0.24221	1.65104	2.445903	2.86135	3.11069
AL ( $\mu_n$ )	360	1044	2088	3492	5256
IR1 ( $\mu_n$ )	8365.41176	22173	40337.6170	62621.72903	88945.7142
IR2 ( $\mu_n$ )	2.98091	2.40416	2.0867263	1.89199	1.761016
IRF ( $\mu_n$ )	2808	7308	13608	21708	31608
IRFW ( $\mu_n$ )	0.8224956	0.63338	0.559033	0.51900	0.49395
IRA ( $\mu_n$ )	3.726372	10.2484	20.376798	34.11134	51.45211
IRB ( $\mu_n$ )	76.11053	230.6625	471.76133	799.406	1213.599
IRC ( $\mu_n$ )	-0.2139701	0.415174	0.594660	0.6678025	0.703944
IRDIF ( $\mu_n$ )	172.48	484.765	962.04684	1604.328	2411.609
IRL ( $\mu_n$ )	177.1077	483.11776	936.65019	1537.70	2286.28
IRLU ( $\mu_n$ )	121.2	344.4	687.6	1150.8	17346
IRLF ( $\mu_n$ )	78.4595263	219.019533	433.06421	720.5935	1081.6076
IRLA ( $\mu_n$ )	71.46036	198.089	390.172	647.7107	970.703
IRGA ( $\mu_n$ )	232.31922	672.94	1350.715	2265.64	3417.71

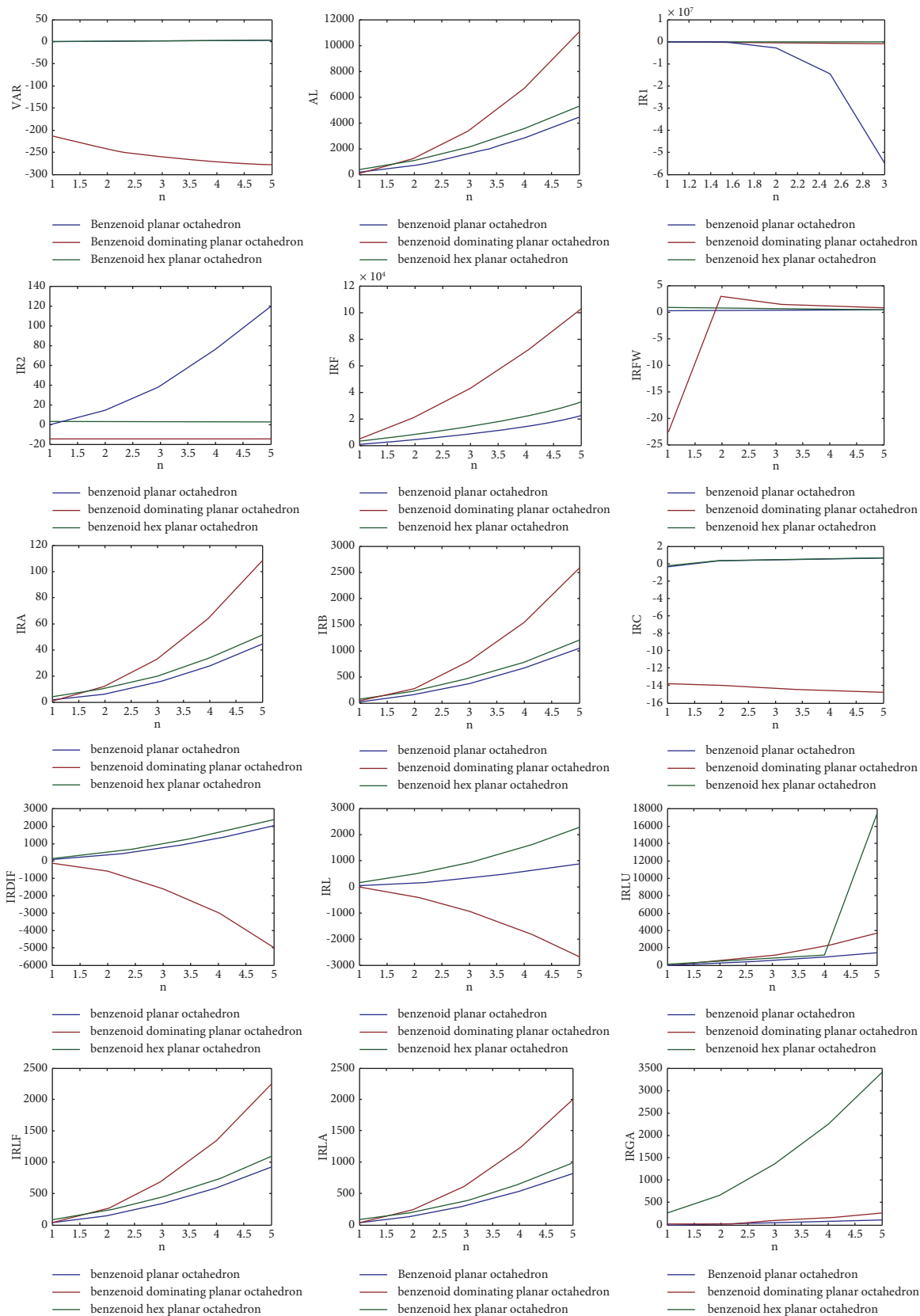
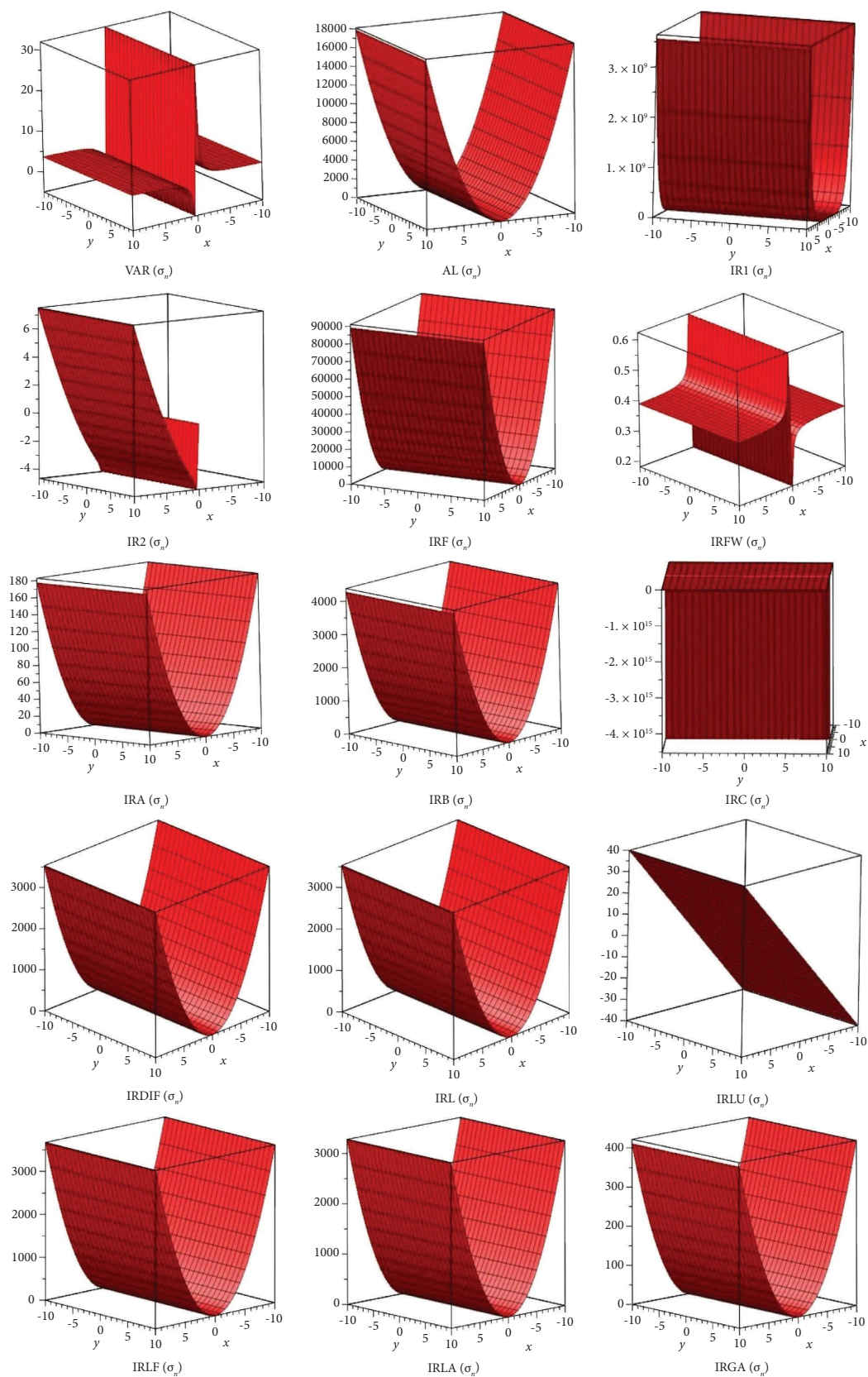


FIGURE 4: 2D plot for irregularity indices of benzenoid planar octahedron structure, benzenoid dominating planar octahedron structure, and benzenoid hex planar octahedron structure.

FIGURE 5: 3D plot for irregularity indices for  $\sigma_n$ .

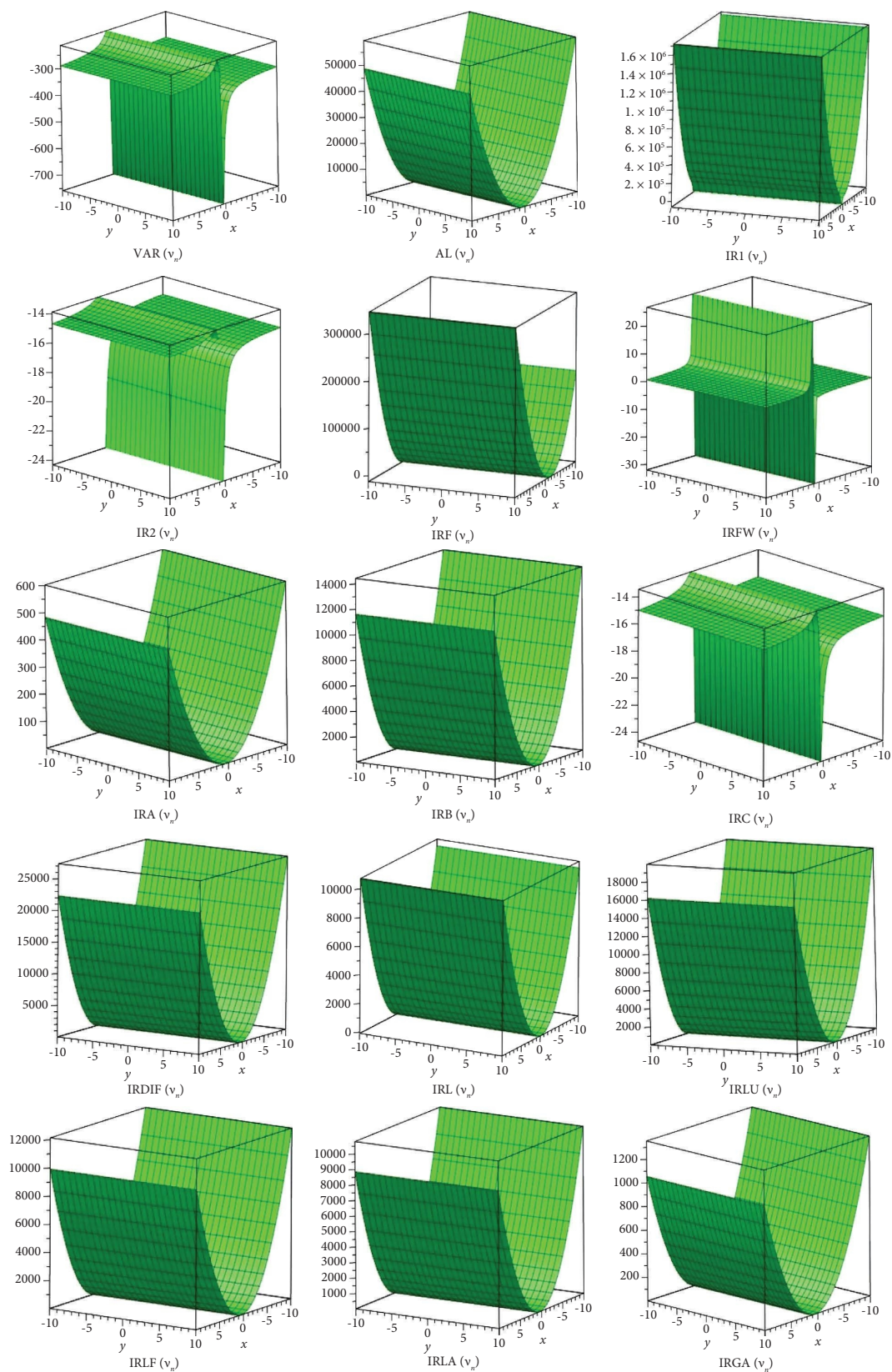
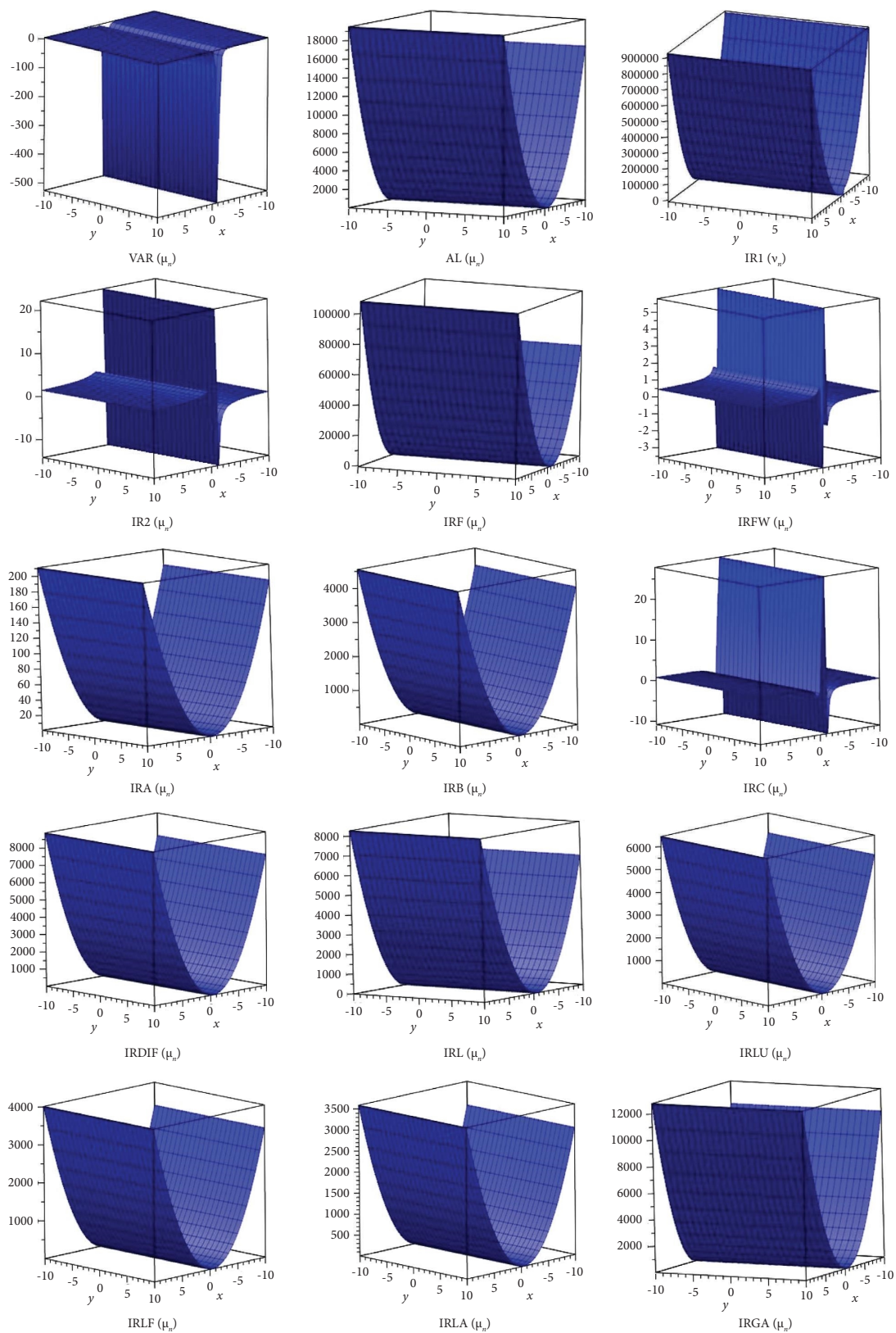


FIGURE 6: 3D plot for irregularity indices for  $\nu_n$ .



FIGURE 7: 3D plot for irregularity indices for  $\mu_n$ .

$$\begin{aligned}
 \text{IRGA}(\mu_n) &= \sum_{lm \in X(\mu)} \ln \frac{\mathfrak{F}(l) + \mathfrak{F}(m)}{2\sqrt{\mathfrak{F}(l)\mathfrak{F}(m)}} \\
 &= (12) \left( \ln \frac{7}{2\sqrt{10}} \right) + (36n^2 - 36n) \left( \ln \frac{6}{2\sqrt{9}} \right) + (24n) \left( \ln \frac{8}{2\sqrt{15}} \right) + (36n^2 + 12n) \left( \ln \frac{11}{2\sqrt{24}} \right) \\
 &\quad + (12n - 6) \left( \ln \frac{10}{2\sqrt{25}} \right) + (12n) \left( \ln \frac{13}{2\sqrt{40}} \right) + (18n^2) \left( \ln \frac{16}{2\sqrt{64}} \right), \\
 &= 118.5759n^2 + 84.894662n + 28.8486661.
 \end{aligned} \tag{8}$$

### 3. Graphical Representation of the Chemical Structures

Here, we differentiate the outcomes of irregularity indices of chemical structures graphically. Three different colours have been exploited to show the graphical behaviour of irregularity indices for chemical structures. These graphs have been existed by substituting the numerical values of  $n$  through the X-axis with respect to the outcomes of irregularity indices through the Y-axis. Tables 4–6 depict such numerical values of outcomes, which can be existed after substituting the numerical values of  $n$ , and these numerical values exhibited in the tables can aid us to make graphical outcomes. Graphical lines with three distinct colours have been employed from Figure 4. Blue colour denotes the behaviour of irregular indices in the Benzenoid planar octahedron structure, red colour denotes the behaviour of irregular indices in the Benzenoid dominating planar octahedron structure, and green colour denotes the behaviour of irregular indices in the Benzenoid hex planar octahedron structure. Numerical values of  $n$  are plotted through the X-axis and two dimensional graphical behaviour of the irregularity indices through the Y-axis are shown in Figure 4. The three dimensional graphical behaviour of the irregularity indices of benzenoid structures are shown in Figures 5–7.

### 4. Conclusion

In the analysis of the quantitative structure property relationships (QSPRs) and (QSARs), chemical indices are important tools to approximate the characteristics of the bioactivity, physical, biomedicine, and chemical compounds. In this paper, we have provided the results on irregularity chemical indices as depicted in Figures 4–7 for Benzenoid planar octahedron structure, Benzenoid dominating planar octahedron structure, and Benzenoid hex planar octahedron structure, besides indices showed increased values for Benzenoid planar octahedron structure, Benzenoid dominating planar octahedron structure, and Benzenoid hex planar octahedron structure. The computational results which we get will aid the investigators to recognise the preferred structure more easily and would inspire the others to concentrate on the Benzenoid planar octahedron structure, Benzenoid dominating planar

octahedron structure, and Benzenoid hex planar octahedron structure.

### Data Availability

All the data and material used in this research is included in the paper.

### Conflicts of Interest

The authors declare that they have no conflicts of interest.

### References

- [1] A. R. Katritzky, R. Jain, A. Lomaka, R. Petrukhin, U. Maran, and M. Karelson, "Perspective on the relationship between melting points and chemical structure," *Crystal Growth & Design*, vol. 1, no. 4, pp. 261–265, 2001.
- [2] A. R. Katritzky, L. Mu, V. S. Lobanov, and M. Karelson, "Correlation of boiling points with molecular structure. 1. A training set of 298 diverse organics and a test set of 9 simple inorganics," *Journal of Physical Chemistry*, vol. 100, no. 24, pp. 10400–10407, 1996.
- [3] H. Wiener, "Structural determination of Paraffin boiling points," *Journal of the American Chemical Society*, vol. 69, pp. 17–20, 1947.
- [4] L. Von Collatz and S. Ulrich, "Spektrien Endlicher Grafen," *Abhandlungen Aus Dem Mathematischen Seminar,* *Der Universitat Hamburg*, vol. 21, no. 1, pp. 63–77, 1957.
- [5] P. L. Krapivsky, S. Redner, and F. Leyvraz, "Connectivity of growing random networks," *Physical Review Letters*, vol. 85, no. 21, pp. 4629–4632, 2000.
- [6] B. Furtula, A. Graovac, and D. Vukićević, "Augmented Zagreb index," *Journal of Mathematical Chemistry*, vol. 48, no. 2, pp. 370–380, 2010.
- [7] M. S. Rosary, "Topological study of Line graph of Remdesivir Compound used in the treatment of corona virus," *Polycyclic Aromatic Compounds*, vol. 42, no. 8, pp. 5731–5747, 2022.
- [8] P. Ali, S. A. K. Kirmani, O. Al Rugaie, and F. Azam, "Degree-based topological indices and polynomials of hyaluronic acid-curcumin conjugates," *Saudi Pharmaceutical Journal*, vol. 28, no. 9, pp. 1093–1100, 2020.
- [9] S. Wazzan and A. Saleh, "Locating and multiplicative locating indices of graphs with QSPR analysis," *Journal of Mathematics*, vol. 2021, Article ID 5516321, 15 pages, 2021.
- [10] R. Todeschini and V. Consonni, *Handbook of Molecular Descriptors, Methods and Principles in Medicinal Chemistry*, Wiley, Hoboken, NJ, USA, 2000.

- [11] I. Gutman and N. Trinajstić, "Graph theory and molecular orbitals. Total pi-electron energy of alternant hydrocarbons," *Chemical Physics Letters*, vol. 17, no. 4, pp. 535–538, 1972.
- [12] M. Randić, "Characterization of molecular branching," *Journal of the American Chemical Society*, vol. 97, no. 23, pp. 6609–6615, 1975.
- [13] T. Reti, R. Sharafzadeh, A. Dregelyi-Kiss, and H. Haghbin, "Graph irregularity indices used as molecular descriptors in QSPR studies," *MATCH Communications in Mathematical and in Computer Chemistry*, vol. 79, pp. 509–524, 2018.
- [14] E. Estrada, "Randić index, irregularity and complex biomolecular networks," *Acta Chimica Slovenica*, vol. 57, no. 3, pp. 597–603, 2010.
- [15] S. Javaraju, A. Alsinai, A. Alwardi, H. Ahmed, and N. D. Soner, "Reciprocal leap indices of some wheel related graphs," *Journal of Prime Research in Mathematics*, vol. 17, no. 2, pp. 101–110, 2021.
- [16] A. Hasan, M. H. A. Qasbi, A. Alsinai, M. Alaeiyan, M. R. Farahani, and M. Cancan, "Distance and degree based topological polynomial and indices of X-level wheel graph," *Journal of Prime Research in Mathematics*, vol. 17, no. 2, pp. 39–50, 2021.
- [17] S. Javaraju, H. Ahmed, A. Alsinai, and N. D. Soner, "Domination topological properties of carbidopa-levodopa used for treatment Parkinson's disease by using  $\phi p$ -polynomial," *Eurasian Chemical Communications*, vol. 3, no. 9, pp. 614–621, 2021.
- [18] Z. Raza, "The expected values of arithmetic bond connectivity and geometric indices in random phenylene chains," *Heliyon*, vol. 6, no. 7, pp. 044799–e4559, 2020.
- [19] X. Zhang, A. Rauf, M. Ishtiaq, M. K. Siddiqui, and M. H. Muhammad, "On degree based topological properties of two carbon nanotubes," *Polycyclic Aromatic Compounds*, vol. 42, no. 3, pp. 866–884, 2020.
- [20] X. Zhang, H. Jiang, J. B. Liu, and Z. Shao, "The cartesian product and join graphs on edge-version atom-bond connectivity and geometric arithmetic indices," *Molecules*, vol. 23, no. 7, pp. 1731–1817, 2018.
- [21] X. Zhang, M. Naeem, A. Q. Baig, and M. A. Zahid, "Study of hardness of superhard crystals by topological indices," *Journal of Chemistry*, vol. 2021, Article ID 9604106, 10 pages, 2021.
- [22] X. Zhang, M. K. Siddiqui, S. Javed, L. Sherin, F. Kausar, and M. H. Muhammad, "Physical analysis of heat for formation and entropy of Ceria Oxide using topological indices," *Combinatorial Chemistry & High Throughput Screening*, vol. 25, no. 3, pp. 441–450, 2022.
- [23] Y.-M. Chu, M. Abid, M. I. Qureshi, A. Fahad, and A. Aslam, "Irregular topological indices of certain metal organic frameworks," *Main Group Metal Chemistry*, vol. 44, no. 1, pp. 73–81, 2021.
- [24] V. Abaid ur Rehman, M. A. Rehman, C. Shi, and W. Nazeer, "Useful Irregularity Indices in QSPR Study for Bismuth Triiodide," *Journal of Chemistry*, vol. 2019, Article ID 2096019, 17 pages, 2019.
- [25] S. Kang, Y. M. Chu, A. R. Virk, W. Nazeer, and J. Jia, "Computing irregularity indices for probabilistic neural network," *Frontiers in Physics*, vol. 8, p. 359, 2020.
- [26] J. Liu, L. Cai, A. R. Virk, W. Akhtar, S. A. Maitla, and Y. Wei, "Computation of irregularity indices of certain computer networks," *Mathematical Problems in Engineering*, vol. 2020, Article ID 2797286, 17 pages, 2020.
- [27] I. Gutman, "Bulletin of the International Mathematical Virtual Institute," *Bibliometric indicators of the Bulletin of IMVI*, vol. 8, pp. 469–475, 2018.
- [28] D. Dimitrov and T. Reti, "Graphs with equal irregularity indices," *Acta Polytechnica Hungarica*, vol. 11, no. 4, pp. 41–57, 2014.
- [29] T. Reti and E. Toth-Laufer, "On the construction and comparison of graph irregularity indices," *Kragujevac J.Sci*, vol. 39, pp. 53–75, 2017.
- [30] M. A. Mohammed, Al, A. R. Virk, and H. Rehman, "Irregularity indices for line graph of Dutch windmill graph," *Proyecciones*, vol. 39, no. 4, pp. 903–918, 2020.
- [31] D. Zhao, Z. Iqbal, R. Irfan et al., "Comparison of irregularity indices of several Dendrimers structures," *Processes*, vol. 7, no. 10, p. 662, 2019.
- [32] B. Furtula and I. Gutman, "A forgotten topological index," *Journal of Mathematical Chemistry*, vol. 53, no. 4, pp. 1184–1190, 2015.
- [33] J. B. Liu, H. Ali, Q. U. Ain, P. Ali, and S. A. K. Kirmani, "On topological properties for benzenoid planar octahedron networks," *Molecules*, vol. 27, no. 19, p. 6366, 2022.